Research paper

Struct Multidisc Optim 26, 37–49 (2004)
DOI 10.1007/s00158-003-0295-6

Examples of density, orientation, and shape-optimal 2D-design for stiffness and/or strength with orthotropic materials

P. Pedersen

Abstract The balance between stiffness and strength design is considered in the present paper. For materials with different levels of orthotropy (including isotropy), we optimize the density distribution as well as the orientational distribution for a short cantilever problem, and discuss the tendencies in design and response (energy distributions and stress directions). For a hole in a biaxial stress field, the shape design of the boundary hole is also incorporated.

The resulting tapered density distributions may be difficult to manufacture, for example, in micro-mechanics production. For such problems a penalization approach to obtain "black and white" designs, i.e. uniform material or holes, is often applied in optimal design. A specific example is studied to show the effect of the penalization, but is restricted here to an isotropic material.

When the total amount of material is not specified, a conflict between optimal design for stiffness and optimal design for strength appears. The computational results of such a case study are shown.

Key words shape design, orientational design, orthotropic materials

1 Introduction

The application of non-isotropic materials is rapidly increasing and it is a challenge for designers to get the most out of the possibilities with new materials. Design for stiffness and for strength are both important, and in addition to the boundary shape and thickness distribution, the material orientation needs to be decided. Laminate design is a specific area of major importance, as shown in the book by Gürdal *et al.* (1999), a book that contains extensive references. In reality, laminate design is more complicated than the problems treated in the present paper.

The goal of the present paper is, by computational results for idealized problems, to provide insight that will also be helpful for more practical cases, in which a number of additional aspects must be taken into account. From general theorems for the case of single-load problems with a given volume of material, we know that designs with a uniform energy density are optimal with respect to stiffness as well as strength (see Pedersen (1998)). Geometrical constraints may give rise to modifications to this statement, and without a volume constraint a direct conflict appears, as is illustrated by an example in the present paper.

The design variables. The paper covers design for thickness (density), design for orientation of orthotropic materials, design of boundary shapes, and combinations of these design variables. The stiffness and strength aspects in relation to a number of specific examples are studied with some or all of these variables, and in applications with different materials.

The materials of the continuum. We describe the material constitutive properties by the tensor components C_{ijkl}, defined according to the stress-strain relation $\sigma_{ij} = C_{ijkl}\epsilon_{kl}$. In addition to an isotropic material with $C_{1122} = 0.3\,C_{1111}$ (Poisson's ratio equal to 0.3), we treat three orthotropic example cases in which the quantities for C_{2222} and C_{1212} are made smaller by dividing by 2, 4, and 8, respectively. Linear elasticity is assumed, but power-law non-linear elasticity would not be more difficult to study (see Pedersen (1998)).

The objectives. Stiffness is a global measure for a whole continuum with volume V. As the objective in stiffness optimization we choose to minimize the total elastic energy U, equivalent to minimization of the compliance.

Strength is a local measure and focus is put on the most critical point(s) in a continuum. As a general meas-

Received: 4 November 2002
Revised version: 11 May 2003
Published online: 25 September 2003

P. Pedersen

Department of Mechanical Engineering, Solid Mechanics Technical University of Denmark, Nils Koppels Allè, Building 404, DK-2800 Kgs.Lyngby, Denmark
e-mail: pauli@mek.dtu.dk

ure for a critical quantity we choose the elastic energy density u ($U = \int_V u \, \mathrm{d}V$), and thus strength optimization involves minimizing the maximum elastic energy density. If a uniform energy density is obtained, then the compliance is stationary, but often geometrical constraints make it impossible to obtain complete uniformity.

For two specific problems, namely a short cantilever and a quarter part of a biaxially loaded hole, with a given total volume we find no conflict between optimal design for stiffness and optimal design for strength, and in general a continuum with a uniform energy density can be determined when the thickness distribution is included as a design parameter. With only orientational design the stiffness can be optimized, but severe energy concentration will still be present. With only shape optimization the domain of uniform energy density is restricted to the designed boundary.

Another example illustrates the influence of penalization to obtain a "black and white" design, i.e. a design of either uniform thickness or holes, as in topology optimization (see Bendsøe and Sigmund (2003)). This study includes the influence of the total amount of material (total material density). Severe energy concentrations are shown to result for a low total material density.

A final example of a loaded cross (connection of two mutually orthogonal rectangular domains) without a volume constraint shows the conflict between optimizing for stiffness and optimizing for strength. Also in this study we find results for different levels of material orthotropy.

The intention of the paper is not to present new theoretical results or new numerical methods, but to get insight from computational solutions to a number of specific problems, all for a single load case and all modelled by the finite element method.

2
Design of thickness or density distribution

The idealized problems of thickness or density design (with stiffness linearly proportional to density) for the largest stiffness have the same solution as the strongest design. The solutions are characterized as continua of uniform energy density as proven also for non-linear elasticity. For reference see Pedersen (1998), which also gives the details behind the sensitivity analysis to follow.

That the results are not restricted to isotropic materials follows from the possibility of a localized determination of the sensitivity in a fixed strain field (or alternatively in a fixed stress field). With U as the total elastic energy, the sensitivity to changes in the thickness (density) t_e in the domain e is

$$\frac{\mathrm{d}U}{\mathrm{d}t_e} = -\left(\frac{\partial(\bar{u}_e V_e)}{\partial t_e}\right)_{\textit{fixed strains}} = -\bar{u}_e \left(\frac{\mathrm{d}V_e}{\mathrm{d}t_e}\right), \qquad (1)$$

where $\bar{u}_e$ is the mean energy density in the domain and V_e is the volume of the domain. Note that *the sensitivity is not physically localized, but we can still determine the localized sensitivity without approximation.*

From this result for sensitivity with a constraint on the total volume, i.e. $\sum_e (\mathrm{d}V_e/\mathrm{d}t_e) = 0$, it follows that the optimality criterion for optimal stiffness is constant energy density:

$$\bar{u}_e = \bar{u}\,, \qquad (2)$$

where $\bar{u}$ is the mean energy density for the whole optimally designed continuum. During design iteration this unknown quantity is estimated by the current mean energy density.

Optimal designs are obtained through a number of iterations. In each iteration a finite element analysis is performed, and based on the information from this analysis (element energy densities) a better design is suggested. The simple recursive formula, in agreement with optimality criteria methods (see Rozvany (1989), Haftka *et al.* (1990), or Bendsøe and Sigmund (2003)), is an update of element thicknesses by

$$(t_e)_{new} = (t_e)_{current} \left(\frac{(\bar{u}_e)_{current}}{\bar{u}_{current}}\right)^{0.8} (\bar{V}/V) \qquad (3)$$

with proper adjustment to limits t_{min} and t_{max} and iteratively updating the current volume V, so that the volume constraint $V = \bar{V}$ is satisfied in each redesign. Alternative procedures to satisfy the volume constraint are possible, but the computational results in the present paper are based on the given formula (3). The relaxation power of 0.8 is used by most researchers but it is not a physical constant. However without this relaxation, design cycling is often observed, while with the relaxation power, monotonic convergence is often obtained. To find the optimized designs we have used 10–20 design iterations, but this number is strongly related to the convergence test, which can be convergence for the objective and/or convergence for the design variables.

The first specific example is a short cantilever with a uniformly distributed load. In addition to an isotropic material we optimize the design based on three different orthotropic materials.

The second example is a biaxially loaded hole with the shape of the hole designed as an ellipse, with the ratio of the axes equal to the ratio of the applied stresses. A uniform energy density is obtained with higher thickness at the hole boundary (re-enforcement), but only within the limits of the maximum thickness, set to five times the mean value.

2.1
Cantilever example of thickness (density) design

The first example is a short cantilever with a uniformly distributed load. In addition to an isotropic material we optimize the design based on three different orthotropic materials. The resulting optimal values are given in Table 1, together with results from only orien-

Table 1 Optimization results for a uniformly loaded short **cantilever**. For isotropy and three cases of orthotropy: results of optimization with combined thickness and orientation, thickness only, and orientation only. The table gives the relative values of the mean energy density (compliance), and the relative values of the maximum energy density The reference value for all the values is the minimum mean energy density

C_{2222}/C_{1111}	C_{1212}/C_{1111}	thickness and orientation		thickness only		orientation only	
		u_{mean}	u_{max}	u_{mean}	u_{max}	u_{mean}	u_{max}
1.00	0.35	1.00	7.12	1.00	7.12	2.19	170
0.50	0.175	1.23	8.75	1.45	12.7	2.55	182
0.25	0.0875	1.71	10.8	2.42	23.4	3.52	204
0.125	0.04375	2.96	11.9	5.73	63.1	8.21	257

tational design and results from combined thickness and orientational design. We wanted to illustrate not only the optimal designs but also the resulting responses (energy density fields and stress directions) for these designs.

Figure 1 presents the collected results for the short cantilever problems, using only thickness optimization. The first row is based on the isotropic material ($C_{2222} = C_{1111}$, $C_{1212} = (C_{1111} - C_{1122})/2$), while the second row corresponds to more flexibility in the vertical direction of the load and in shear ($C_{2222} = C_{1111}/2$, $C_{1212} = (C_{1111} - C_{1122})/4$). The third row corresponds to even more flexibility ($C_{2222} = C_{1111})/4$, $C_{1212} = (C_{1111} - C_{1122})/8$) and the fourth row corresponds to extreme flexibility in the direction of the loads and in shear ($C_{2222} = C_{1111}/8$, $C_{1212} = (C_{1111} - C_{1122})/16$).

For each solution two pictures are found necessary in addition to the tables of obtained relative values. The images to the left show examples of the first kind of picture. Colour-plots are naturally more informative, but the explanation here is related to the grey-scale in Fig. 1. The scale illustrate values of the *ratio of principal stresses* $-1 \leq \sigma_2/\sigma_1 \leq 1$, where dark areas correspond to extreme values ($\sigma_2 = -\sigma_1$, i.e. pure shear stress) or ($\sigma_2 = \sigma_1$, i.e. isotropic stress) while light areas correspond to unidirectional stress ($\sigma_2 = 0$). In the images to the left *supports* at the left are shown by arrow heads and it is noted that

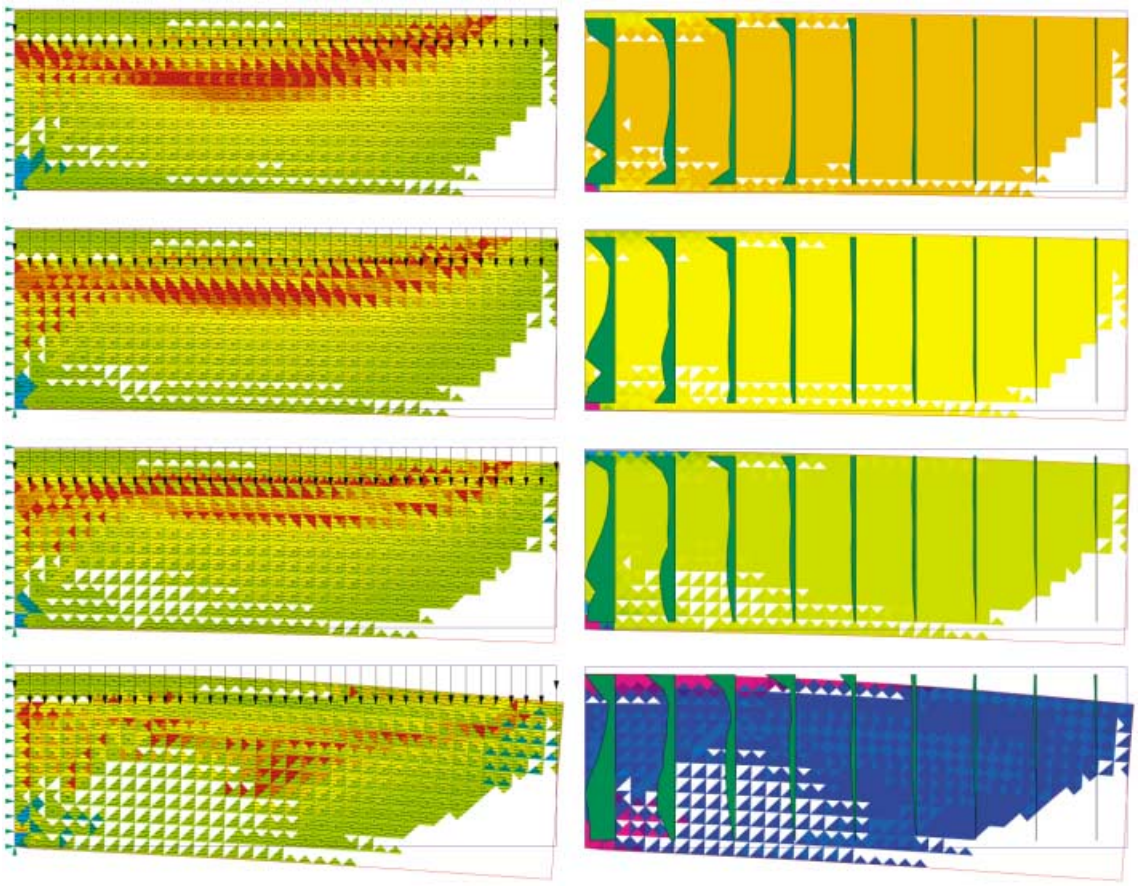

Fig. 1 Cantilever results with only thickness design. The first row: isotropic. The second row: 50% C_{2222}, C_{1212} (compared with the isotropic case). The third row: 25% C_{2222}, C_{1212}. The fourth row: 12.5% C_{2222}, C_{1212}

the vertical support is concentrated on a single node, thus resulting in energy concentration at that node. *Loads* are the forces equivalent to a uniform load and are shown to be acting on the non-deformed upper part. The hatching shows the *material orthotropic direction* and, if optimal, also the *principal stress direction*.

In the pictures to the right, the *thickness (density) distribution* is shown by nine cross-sectional cuts on top of a grey-scale for the resulting *energy density field*. The white spots indicate the resulting thicknesses at the minimum value ($t_{minimum} = 0.001 t_{mean}$), and thus can be interpreted as *"holes"*. Note that these holes also relate to the finite element modelling, with each quadrangle divided into four constant-stress triangles. Furthermore, no filtering (smoothing) to avoid checkerboard solutions is performed (see again Bendsøe and Sigmund (2003)). A maximum thickness ($t_{maximum} = 5 t_{mean}$) is also prescribed.

The designs can be seen as comprising three main domains: an outer part where the inactive corner disappears while the remaining outer part has almost uniform thickness; a middle part where the design tends toward an I-beam; and an inner part dominated by the specified singular support where a concentration of energy density is still active.

From the pictures to the right we see that all four cases result in an almost uniform distribution of energy density, and thus are optimal with respect to stiffness as well as to strength. The different uniform grey levels are due to an increasing level of energy density when the stiffness of the material is decreased. The different levels of the (magnified) displacements also illustrate this fact. Especially with the most flexible material we see the influence of the finite element modelling, with domains in a triangular checkerboard pattern. We note that, especially at the support, the optimal thickness distribution changes with the level of orthotropy.

Note, furthermore, from the pictures to the left that with the materials that are more flexible in shear, the areas (dark areas) of resulting pure shear stress diminish.

2.2 Biaxially loaded hole example of thickness (density) design

Figure 2 shows the results for the second continuum example, the biaxially loaded hole problem. We present the results again for the same four different materials as used for the cantilever example, and with only thickness (density) optimization. The boundary shape is given as an ellipse, with the ratio of the axes equal to the ratio of the external loads ($a/b = 3/2$). Results for the shape and orientational designs are shown later in Sects. 3 and 4.

The results in the pictures to the right show a reenforcement of the hole boundary and we obtain an almost uniform energy density. Again for the materials with lower shear stiffness, the design tries to minimize areas of resulting pure stresses. The dark areas in the pictures to the left correspond to areas of resulting isotropic stress, and in the remaining parts almost unidirectional stresses result.

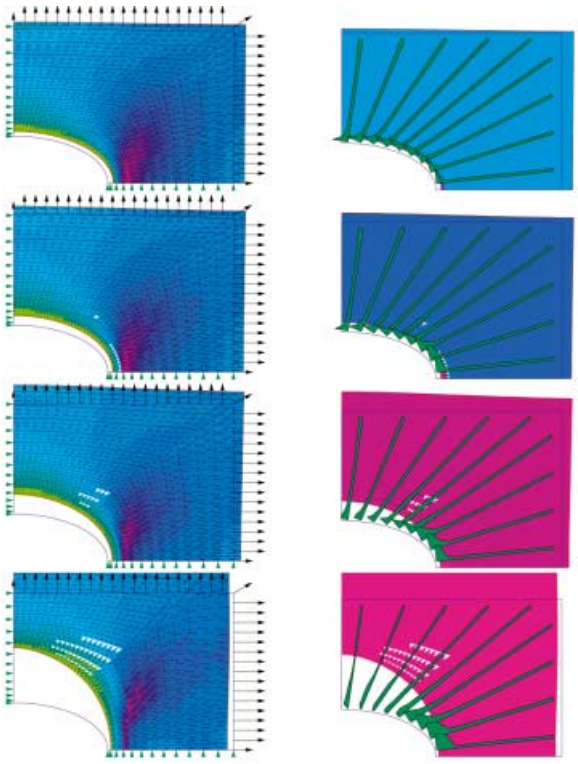

Fig. 2 Hole problem results with only thickness design. The first row: isotropic. The second row: 50% C_{2222}, C_{1212} (compared with the isotropic case). The third row: 25% C_{2222}, C_{1212}. The fourth row: 12.5% C_{2222}, C_{1212}

3 Design of orientational field

The optimality criterion for orientational design is given by the alignment of directions of orthotropy, principal stress, and principal strain (see Cheng and Pedersen (1997) and, for exceptions, Pedersen (1989)). Restricted to cases in which this alignment is valid, solutions for the stiffest design are shown. It is noted that the problem of the strongest design is not covered by these solutions, and in general thickness design is necessary to eliminate energy concentration.

Results of the influence of the level of orthotropy on the orientation field of the optimal design are presented. Combinations with thickness optimization are also illustrated.

Optimal designs are again obtained through a number of iterations. In each iteration a finite element analysis is performed, and based on the information from this analysis (element principal stress direction for the numerically larger principal stress) a better design is suggested. The simple recursive formula in agreement with the optimality criterion is an update in each element of the stiffest

material direction to align with the principal stress direction. Fast convergence is found both with orientational design alone and in combination with thickness design, which means that the same finite element analysis is used for both orientational re-design and thickness re-design.

3.1
The two examples with only orientational design

The examples are the same as for the pure thickness optimization, which means that the importance of the orientational design can be evaluated.

In Fig. 3 for the cantilever examples we note in the pictures to the left that the dark area corresponding to pure shear stress diminishes in the designs based on materials that are more flexible in shear, and we end up with almost unidirectional stress everywhere in the cantilever. In the pictures to the right we see severe concentration of energy density and thus the orientational optimization alone is not able to eliminate the drastic values in Table 1 for stress concentration.

In Fig. 4 for the hole examples the energy concentrations are not eliminated either, but due to the relatively good shape design the values in Table 2 are more moderate. In the pictures to the left we see that an almost

Table 2 Optimization results for a biaxially loaded quarter of a **hole**. For isotropy and three cases of orthotropy: results of optimization with combined thickness and orientation, thickness only, and orientation only. The table gives the relative values of the mean energy density (compliance), and the relative values of the maximum energy density The reference value for all the values is the minimum mean energy density

C_{2222}/C_{1111}	C_{1212}/C_{1111}	thickness and orientation		thickness only		orientation only	
		u_{mean}	u_{max}	u_{mean}	u_{max}	u_{mean}	u_{max}
1.00	0.35	1.00	1.53	1.00	1.53	1.05	3.61
0.50	0.175	1.05	1.59	1.13	2.46	1.10	4.18
0.25	0.0875	1.14	1.51	1.42	4.28	1.18	4.34
0.125	0.04375	1.25	1.92	2.72	9.72	1.33	6.68

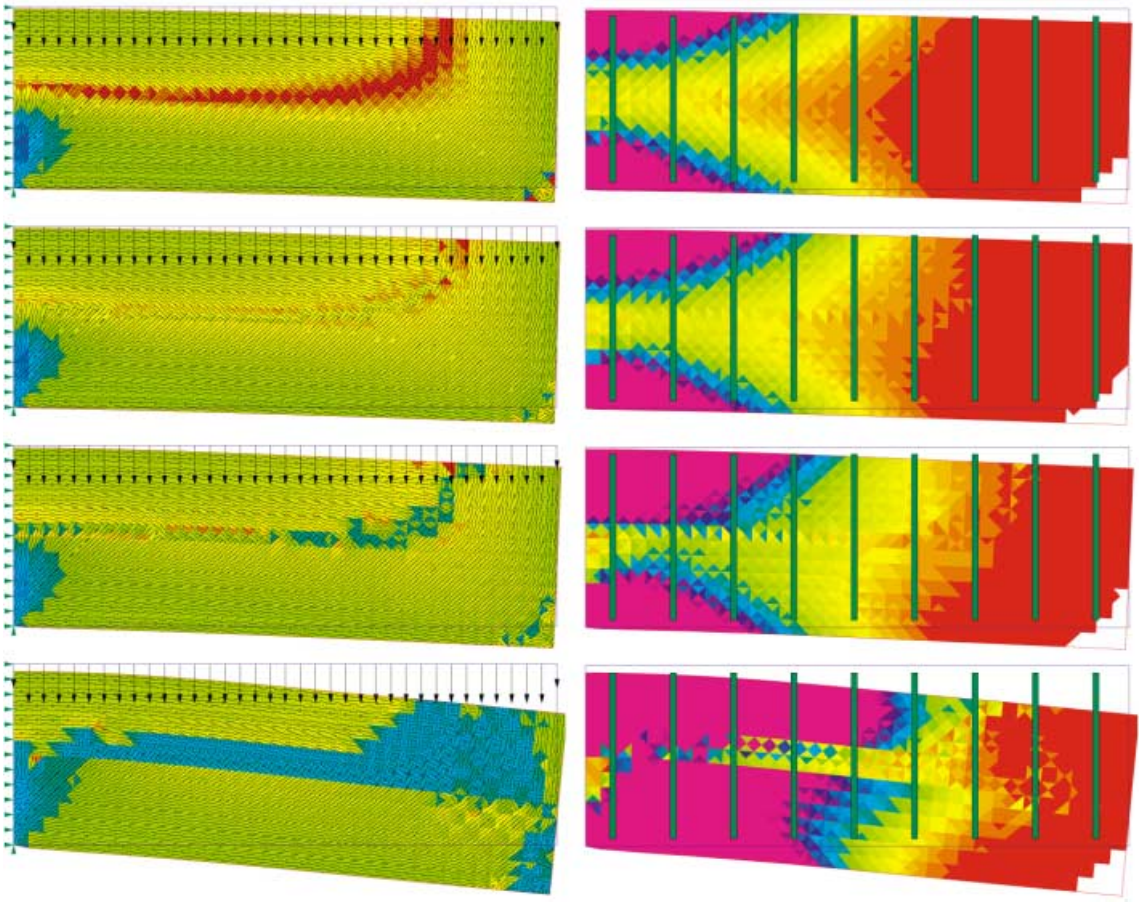

Fig. 3 Cantilever results with only orientational design. The first row: isotropic. The second row: 50% C_{2222}, C_{1212} (compared with the isotropic case). The third row: 25% C_{2222}, C_{1212}. The fourth row: 12.5% C_{2222}, C_{1212}

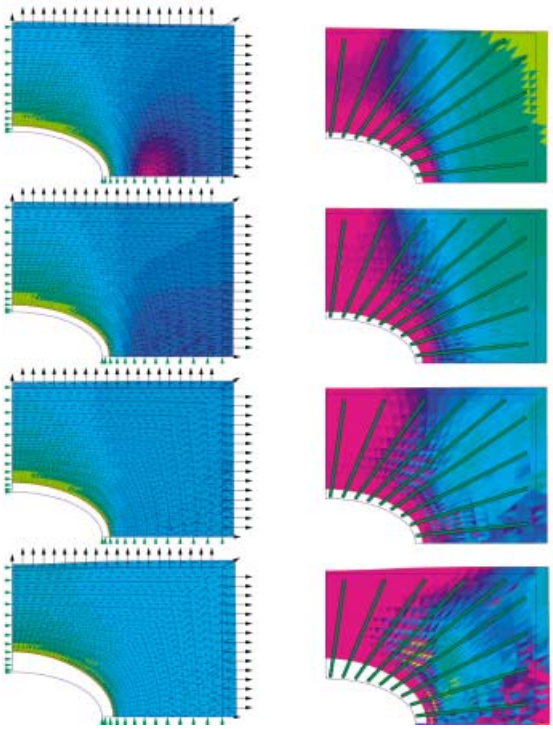

Fig. 4 Hole problem results with only orientational design. The first row: isotropic. The second row: 50% C_{2222}, C_{1212} (compared with the isotropic case). The third row: 25% C_{2222}, C_{1212}. The fourth row: 12.5% C_{2222}, C_{1212}

unidirectional state of stress is obtained for the strongly orthotropic materials. The dark areas for the isotropic case (upper left corner picture) do not correspond to pure shear stress ($\sigma_2 = 0$) but to the other extreme (isotropic stresses ($\sigma_2 = \sigma_1$). The pictures to the right in Fig. 4 show non-uniform energy densities, which naturally result when thickness optimization is not included. Because of the elliptical boundary shape a severe concentration is not found.

The general conclusion is that stiffness can be improved by orientational design, but for strength optimization we need the thickness design. On the other hand the orientational design will influence the resulting thickness design. The resulting optimal values are given in Table 1 and 2.

3.2
The two examples with combined thickness and orientational design

In Table 1 for the cantilever examples and in Table 2 for the hole problem, we have collected values for the relative stiffness (compliance) described by u_{mean} and values for the relative energy concentrations described by u_{max}. These results are for the thickness-only optimizations, for the orientational-only optimizations, and for the combined optimizations.

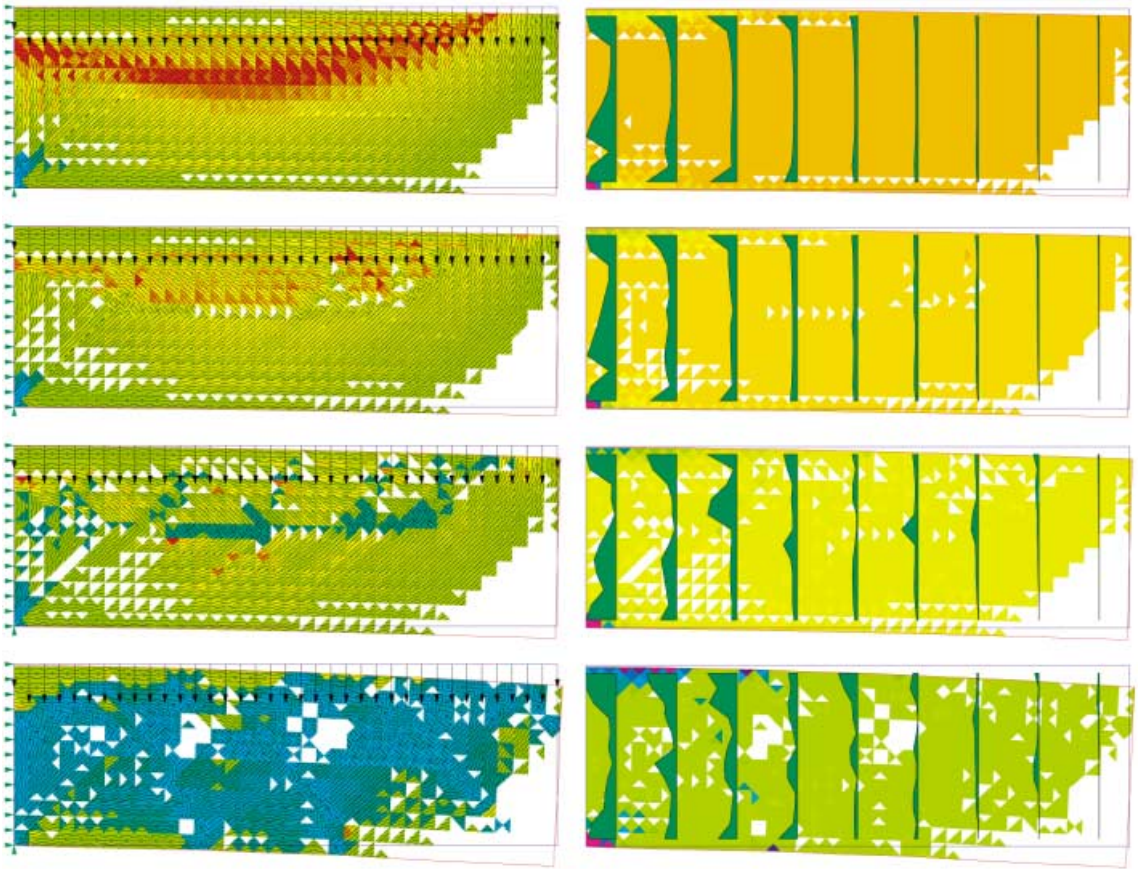

Fig. 5 Cantilever results with both thickness and orientational design. The first row: isotropic. The second row: 50% C_{2222}, C_{1212} (compared with the isotropic case). The third row: 25% C_{2222}, C_{1212}. The fourth row: 12.5% C_{2222}, C_{1212}

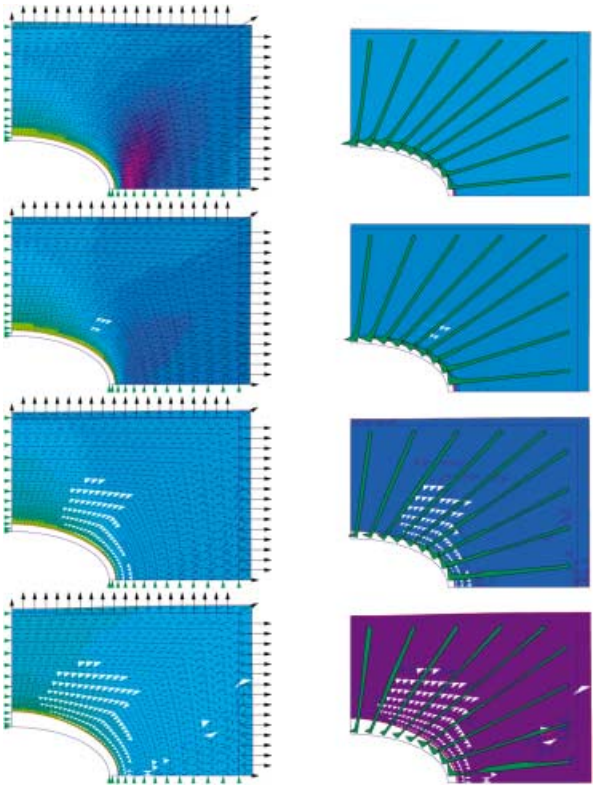

Fig. 6 Hole problem results with both thickness and orientational design. The first row: isotropic. The second row: 50% C_{2222}, C_{1212} (compared with the isotropic case). The third row: 25% C_{2222}, C_{1212}. The fourth row: 12.5% C_{2222}, C_{1212}

For these combined optimizations the resulting optimal cantilevers and their corresponding energy distributions are shown in Fig. 5. The pictures to the left of the ratio of principal stresses and material (stress) directions again show the tendency to obtain unidirectional stresses for the orthotropic materials. In the pictures to the right uniform energy densities are obtained. The optimal thickness distributions depend a lot on the level of orthotropy. However, the results for the preselected cross-sectional cuts are influenced by the increasing number of holes. Further constraints on the thickness (density) variations might be a subject for a further study.

In Fig. 6 the results for the hole problems are shown, and in general the conclusions are the same as for the cantilever problems. In Sect. 4 we include the shape of the boundary as a design variable, and still keep the total volume of the material constant.

4
Shape design of boundary

When geometrical constraints are not active, then a boundary shape with a constant energy density gives both the best stiffness and the best strength (see Pedersen (1998) and Pedersen (2001)). Based on this optimality criterion we can find optimal shapes, and it is proven in these papers that this also holds for non-isotropic materials.

The optimal shape depends strongly on the level of orthotropy, which is also illustrated in Pedersen *et al.* (1992).

4.1
The numerical procedure and example

With the simple super-elliptic parameterization

$$\left(\frac{x_1}{a}\right)^{\eta} + \left(\frac{x_2}{b}\right)^{\eta} = 1 \tag{4}$$

the optimization of the boundary shape for the biaxially loaded hole is more or less a parameter study, mainly in the super-ellipse parameter η. The ellipse axes are a and b and in Pedersen (2000) an optimality criterion related to the parametrization in a, b, η is presented.

In addition to the thickness and orientational optimization for the hole we optimize the boundary shape with a constraint on the area of the hole. It is noted that the ratio of the ellipse axes will change with the level of

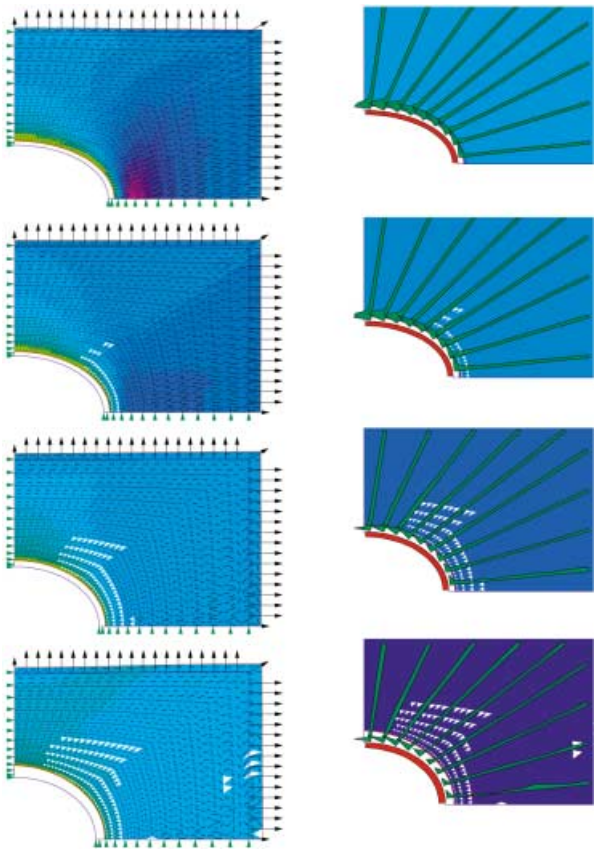

Fig. 7 Hole problem results with shape, thickness, and orientational design. The first row: isotropic. The second row: 50% C_{2222}, C_{1212} (compared with the isotropic case). The third row: 25% C_{2222}, C_{1212}. The fourth row: 12.5% C_{2222}, C_{1212}. In the pictures to the right, the thicknesses of the dark areas along the hole boundaries are a measure of the local energy density

orthotropy, as is also reported in Pedersen *et al.* (1992), where the thickness and orientation are fixed. The results for the three orthotropic cases in Table 2 for (u_{mean}, u_{max}) are (1.05, 1.59), (1.14, 1.51), and (1.25, 1.92), respectively, are improved with the optimized shape to (1.04, 1.30), (1.13, 1.36), and (1.22, 1.59), respectively.

Figure 7 illustrates the results with the same technique as in Figs. 2 and 4. In the pictures to the right, information is added about the variation of the energy density along the hole boundary. The thickness of the dark areas along the hole boundary is a measure of the local energy density, and the uniformity thus confirms that a uniform energy density is obtained along the hole boundary.

Even for the isotropic material (the top pictures in Fig. 7), the optimal ratio of the ellipse axes is not equal to the ratio of the applied stresses. The classical result only holds for infinite domains (small holes) and the solution clearly shows this. For this case the reference values in Table 2 for (u_{mean}, u_{max}) are (1.00, 1.53) with an energy concentration of 53% even after thickness optimization. With shape optimization the ratio of the ellipse axes is changed from 6/3 to 5.6/3.2 (constant area), and the values of (u_{mean}, u_{max}) are then (0.99, 1.29). The conclusion is that the shape optimization has little influence on the overall stiffness, but the shape optimization is important for the concentration of energy density (stress concentration factor for the latter case will only be $\sqrt{1.29} \cong 1.14$).

5
The effect of penalizing in topology optimization

To obtain a "black and white" design, the intermediate densities must be penalized. A frequently used technique to achieve this end is to modify the expression for the elastic energy U to

$$U = \sum_e u_e(t_e)^q \,, \tag{5}$$

where q is some power (often $q = 3$ is chosen). The sensitivity of this objective follows from (1):

$$\frac{\mathrm{d}U}{\mathrm{d}t_e} = -\left(\frac{\mathrm{d}U}{\mathrm{d}t_e}\right)_{\textit{fixed strains}} = -u_e q (t_e)^{q-1} \,. \tag{6}$$

We find that if $u_e(t_e)^{q-1}$ is constant, then the stationarity condition for compliance is fulfilled.

The literature for methods to solve this modified problem is rich, both with respect to the necessary specific methods and obtained designs (see Bendsøe and Sigmund (2003) and the references therein). In fact, for the solution, the methods of mathematical programming are used more than the optimality criteria methods applied in this paper. With methods of mathematical programming several constraints can be incorporated.

5.1
An illustrative example

We solve in a simple manner with an optimality criterion a specific example for different total amounts of material, and discuss the resulting designs with and without penalized intermediate densities. The figures within this section are different from the previous ones. To the right we show designs, and to the left we show the response in terms of the square root of energy densities (stress level). The upper parts of Figs. 8, 9, 10, and 11 correspond to optimal designs without penalization, and the lower parts correspond to optimal designs with penalization (uniform thickness and holes).

Figures 8, 9, 10, and 11, and Table 3 show the results of the specific problem, solved with a simple heuristic approach, based on the optimality criterion $u_e(t_e)^{q-1} = \textit{constant}$, comparing solutions with $q = 3$ and $q = 1$, i.e. with and without penalizing. To be specific we use in all cases 16 iterations with $q = 1$, followed by 16 iterations with $q = 3$. The solutions are stable after these 16 iterations.

We find a strong influence from the penalization, and *the "black and white" designs are obtained at the cost of lower stiffness and higher stress concentration.* This is not surprising, but it gives insight for comparing the results.

It should be noted that the total volume is kept the same in all the examples , and furthermore, that the stiffness analyses are based on the thicknesses used, and not on the penalized thicknesses, which are only used for the redesign procedure (this is not the case in most topology optimization programs). On the optimized black

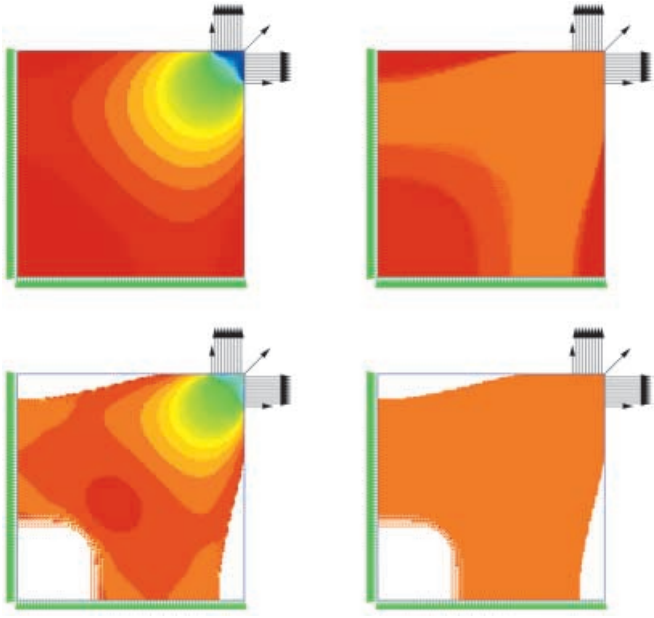

Fig. 8 Results for 80% material usage. Left: square root of energy densities. Right: Optimal designs. Upper: not penalized with $0.001 \leq t_e \leq 1.25$ (corresponding to 80% with $1.25 \times 0.8 = 1$). Lower: penalized to "black and white"

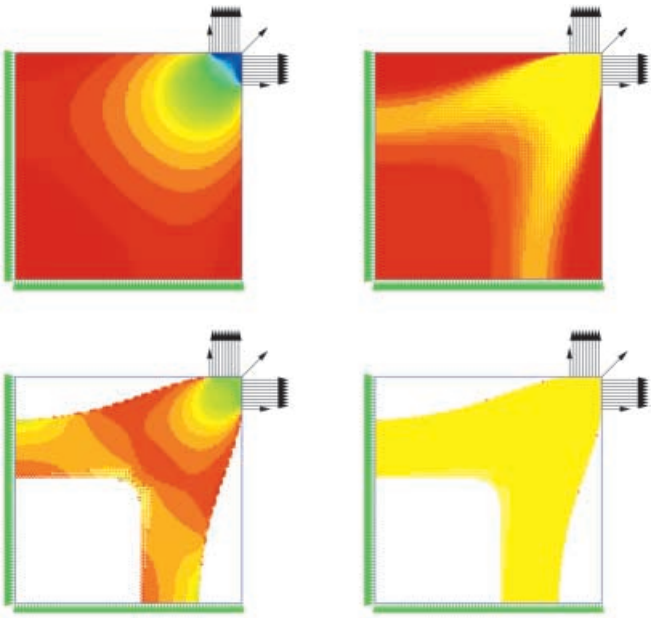

Fig. 9 Results for 50% material usage. Left: square root of energy densities. Right: Optimal designs. Upper: not penalized with $0.001 \leq t_e \leq 2$ (50%). Lower: penalized to "black and white"

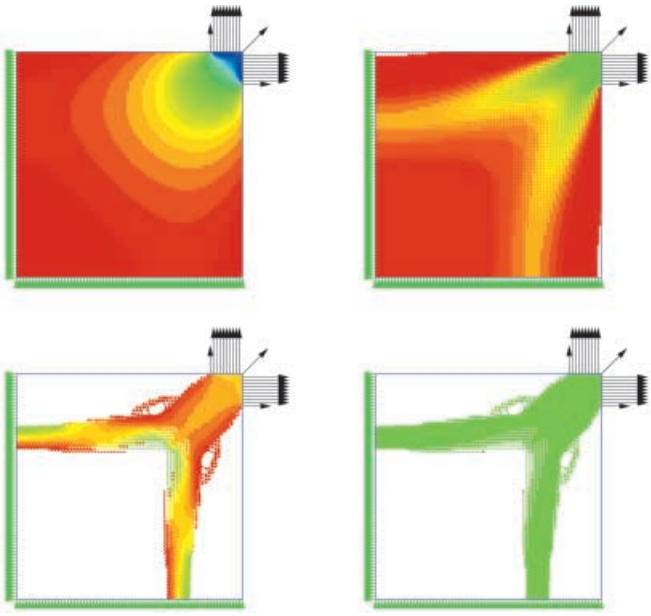

Fig. 10 Results for 25% material usage. Left: square root of energy densities. Right: Optimal designs. Upper: not penalized with $0.001 \leq t_e \leq 4$ (25%). Lower: penalized to "black and white"

and white designs, where the densities are either zero or one, this will not make any difference. Also it should be mentioned that the thicknesses are not scaled to the range of zero to one, but a common scaling factor does not change the penalization.

Figures 8, 9, 10, and 11 show the results of optimal design with given boundary stresses. For the four different figures, relative maximum densities of 1.25, 2, 4, and 8, respectively, were chosen, corresponding for the penalized

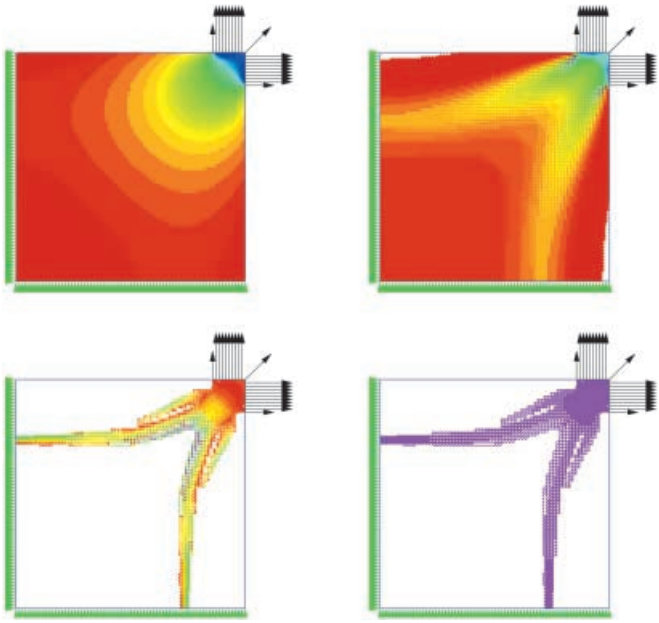

Fig. 11 Results for 12.5% material usage. Left: square root of energy densities. Right: Optimal designs. Upper: not penalized with $0.001 \leq t_e \leq 8$ (12.5%). Lower: penalized to "black and white"

cases to total relative densities of 80%, 50%, 25%, and 12.5%. Table 3 gives the relative values for the compliance (measured by u_{mean}) and for the stress concentration (measured by u_{max}). The finite element model has 19 600 constant stress triangular elements and a total of 19 882 degrees of freedom with a bandwidth of 284:

a) The uniform design is used as a reference for all the cases, and for this we find a stress concentration factor equal to 22.7, active in the loaded corner as seen in the

Table 3 Table of relative values for the solutions shown in Figs. 8, 9, 10, and 11

Constraints	Design	u_{mean}	u_{max}	Note
	Uniform	1.00	22.7	a)
$0.001 \leq t_e \leq 1.25$ $q = 1$	Optimized not penalized	0.86	14.5	b)
$0.001 \leq t_e \leq 1.25$ $q = 3$ and 80%	Optimized penalized	0.90	14.5	c)
$0.001 \leq t_e \leq 2.00$ $q = 1$	Optimized not penalized	0.71	5.43	d)
$0.001 \leq t_e \leq 2.00$ $q = 3$ and 50%	Optimized penalized	0.84	12.3	e)
$0.001 \leq t_e \leq 4.00$ $q = 1$	Optimized not penalized	0.65	1.28	f)
$0.001 \leq t_e \leq 4.00$ $q = 3$ and 25%	Optimized penalized	1.02	36.2	g)
$0.001 \leq t_e \leq 8.00$ $q = 1$	Optimized not penalized	0.65	0.68	h)
$0.001 \leq t_e \leq 8.00$ $q = 3$ and 12.5%	Optimized penalized	2.44	129.3	i)

upper left picture of all the Figs. 8, 9, 10, and 11, with a colour scale proportional to the square root of the element energy density, (i.e. proportional to stresses).

b) For a maximum density that is only 25% higher than the mean density, not much can be obtained by optimal design. Figure 8 shows this. Accepting intermediate densities ("grey" design) we improve the compliance from 1.00 to 0.86 and the stress concentration from 22.7 to 14.5.

c) The same case as in b) but now penalized to obtain a "black and white" design. The lower part of Fig. 8 shows this design to the right, with its resulting distribution of energy density to the left. The numbers are almost the same as those for the "grey" design with the compliance improved to 0.90 and the stress concentration equal to 14.5.

d) For a maximum density double the mean density, the optimal designs are presented in Fig. 9. Accepting intermediate densities ("grey" design) we improve the compliance from 1.00 to 0.71 and especially the stress concentration is improved from 22.7 to 5.43.

e) The same case as in d) but now penalized to obtain a "black and white" design. The lower part of Fig. 9 shows this design to the right, with its resulting distribution of energy density to the left. The results are now different from those for the "grey" design with the compliance only improved to 0.84 and the stress concentration still high and equal to 12.3.

f) For a maximum density equal to four times the mean density, the optimal designs are presented in Fig. 10. Accepting intermediate densities ("grey" design) we improve the compliance almost to the limit, from 1.00 to 0.65 and the stress concentration is then controlled from 22.7 to 1.28, but is still active.

g) The same case as in f) but now penalized to obtain a "black and white" design. The lower part of Fig. 10 shows this design to the right, with its resulting distribution of energy density to the left. The compliance is no longer improved, but almost unchanged from 1.00 to 1.02, and the stress concentration is now increased to 36.2. However, this is partly due to the finite element modelling of the resulting complicated design and boundary smoothing could be effective. So the design in the lower right of Fig. 10 must be post-processed.

h) For a maximum density equal to eight times the mean density, the optimal designs are presented in Fig. 11. Accepting intermediate densities ("grey" design) we improve the compliance almost to the limit, from 1.00 to 0.65 and the stress concentration is then almost completely eliminated from 22.7 to 0.68. We know that without size constraints the optimal design has a uniform energy density, and see that this is almost obtained. The practical question then is related to the modelling accuracy with high density gradients at the loaded corner, as seen in the upper right of Fig. 11.

i) The same case as in h) but now penalized to obtain a "black and white" design. The lower part of Fig. 11 shows this design to the right, with its resulting distribution of energy density to the left. The compliance is now changed from 1.00 to 2.44, and the calculated stress concentration is 129.3. However, this is partly due to the finite element modelling of the resulting complicated design.

Thus, for the examples with "black and white" solutions we need post-processing with, for example, shape design variables.

We have studied the influence of penalization, but without incorporating more advanced procedures with filtering (smoothing) and continuation techniques. We used many simple constant stress triangular elements (19 600) and used optimality criterion methods as an alternative to other topology optimizations. The results are as expected and comparisons with alternatively obtained solutions will be interesting.

6 The balance between optimization for stiffness and optimization for strength

In the examples discussed until now the total amount of material has been given, and in general we find no con-

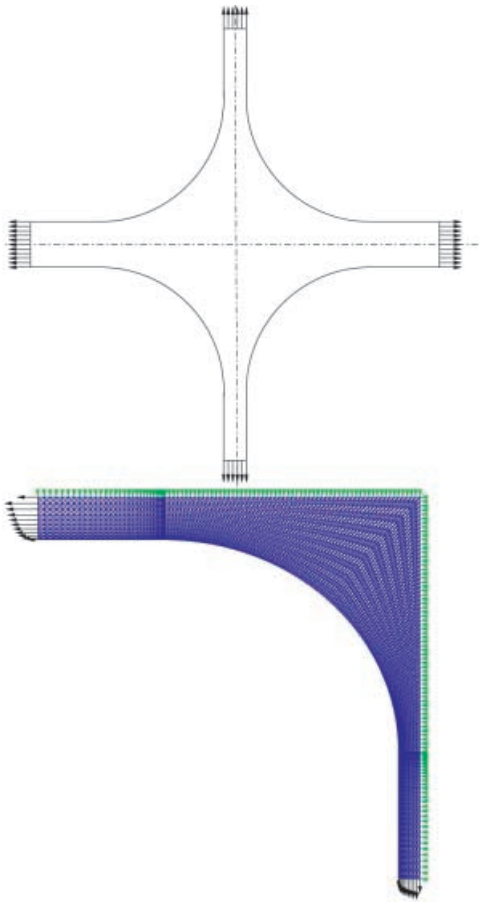

Fig. 12 Top: total model for the cross design problem with ratio of the uniform width of the arms = 2/1, and equal uniform external stress load. Bottom: finite element model based on symmetry using 7200 elements

flict between optimizing for stiffness and optimizing for strength. We now show an example without a material constraint to illustrate a conflict between stiffness and strength.

Figure 12 shows a model of a stress problem for a connection between mutually orthogonal rectangular domains (a cross). The model is shown in full and so is the numerical finite element model for the quarter part, for which the double symmetry has been used. At first only the shape of the curved boundary between the straight sided arms will be our design variable.

As for the hole problem we describe this shape as a super-ellipse (4) with the given axes of the super-ellipse, and thus only have a single parameter. In Fig. 12 this parameter is two ($\eta = 2$) and therefore the shape is an ordinary ellipse, which we use as a reference for values of the compliance, energy concentration, and material volume.

Animation results with η as the changing parameter give good insight into the change, not only of the specific values for the compliance, energy concentration, and material volume, but also into the design response more generally. We want to optimize the parameter η in order to minimize the maximum energy density. In Fig. 13 we present results only for $\eta = 2$ and for the η value that minimizes the energy concentration, i.e. maximizes the strength of the cross.

The two top pictures are for the isotropic material with the reference design to the left, showing an energy concentration of 30.4%. The dark areas around the contour of the model show how the energy density varies and makes it more easy to locate the spots of concentration, which are close to the transitions in the design from a straight line into a curved ellipse.

The top picture to the right shows that a relatively large amount of material is removed, with the total volume of the transition zone (without the "arms") now being only 67% and the energy concentration being improved from 30.4% to 13.8%. However, the compliance of the continuum increases by 20.9%. Thus the designer must choose between stiffness and strength, or alternatively assign a constraint to one of them and then optimize the other one.

The bottom two pictures show the same results for an orthotropic material with decreased stiffness in the vertical (x_2) direction and in shear to 50% of the isotropic

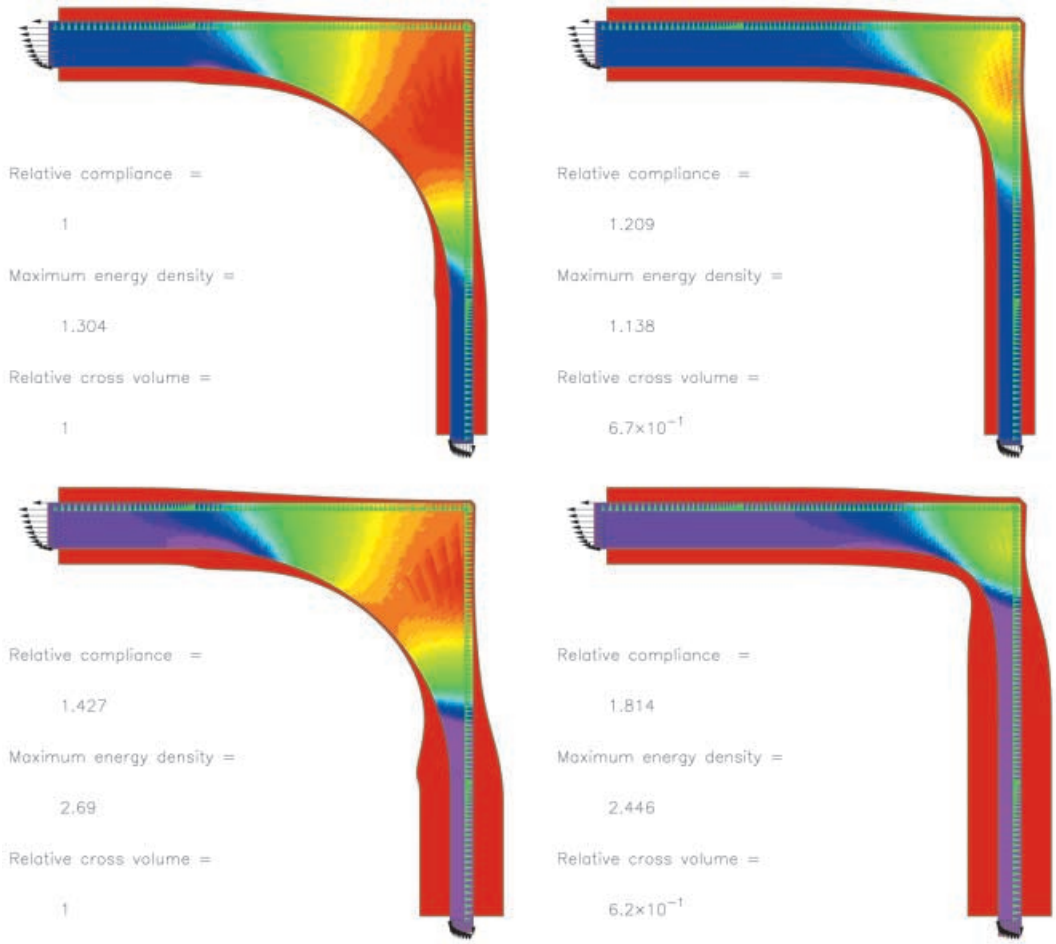

Fig. 13 Top: cross designs for an isotropic material. Bottom: cross designs for 50% C_{2222}, C_{1212} (compared with the isotropic material), here without orientational design. Optimization for strength to the right and elliptic shape to the left. No volume constraint. The thicknesses of the dark areas along the boundaries are a measure of the local energy density

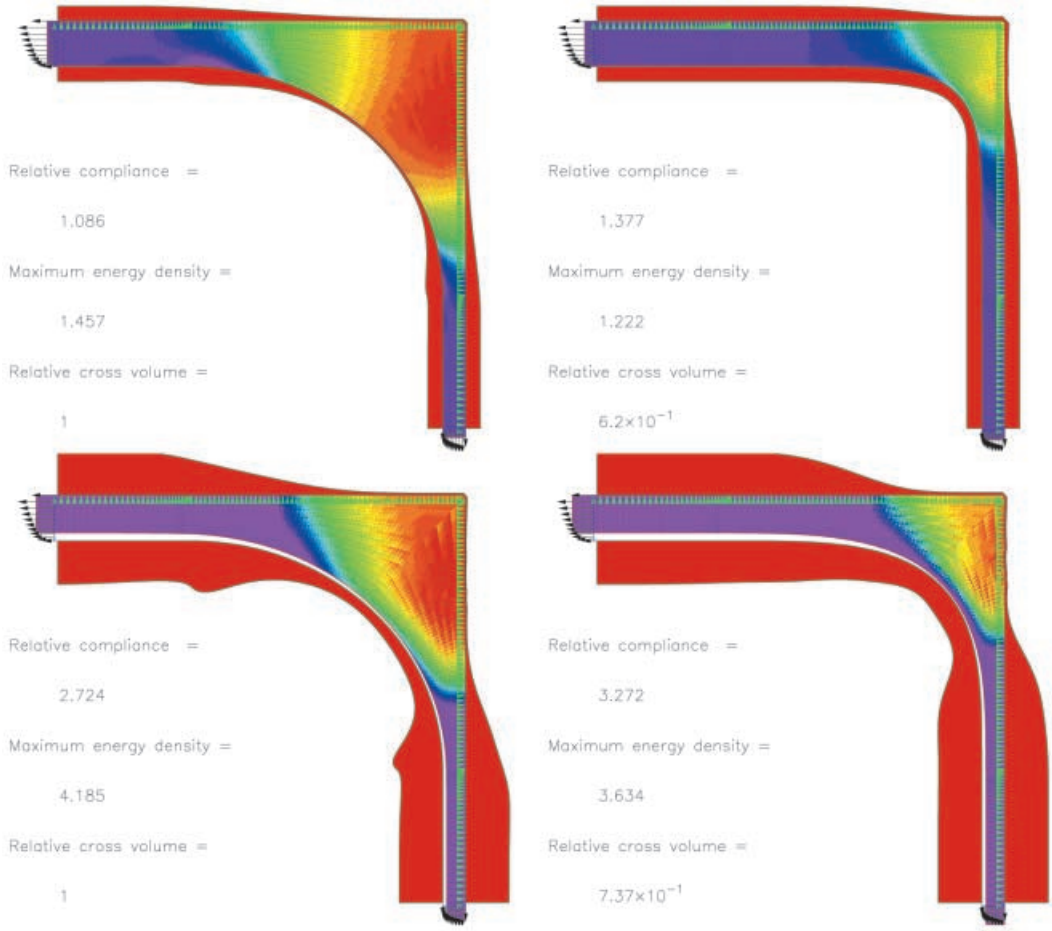

Fig. 14 Top: cross designs for 50% C_{2222}, C_{1212} (compared with the isotropic material), here with orientational design. Bottom: cross designs for 12.5% C_{2222}, C_{1212} material with orientational design. Optimization for strength to the right and elliptic shape to the left. No volume constraint. The thicknesses of the dark areas along the boundaries are a measure of the local energy density

values. Relative to the isotropic case the compliance increases by 42.7% as a result of this more flexible material. The energy concentration is now especially severe, with a factor 2.69, compared with 1.304.

Optimal shape design, as shown in the bottom picture to the right, improves the energy concentration only slightly from 2.69 to 2.446, with a volume decrease to 62%, but at the expense of an increase in compliance from 1.427 to 1.814. For such an orthotropic material the orientational design in addition to shape optimization is of vital importance, as shown in Fig. 14.

In Fig. 14 the internal dark hatchings indicate the directions of the stiffest material directions, aligned with the larger principal stress directions. The top pictures are based on the same material as the bottom pictures in Fig. 13, but here the orientational optimization is added. This improves, for the ellipse design, the compliance from 1.427 to 1.086 and the energy concentration from 2.69 to 1.457, with values now close to the isotropic, more stiff material. We may say that the increased material flexibility is to a large extent compensated by orientational design. Also the values for the optimized shape are close to the values for the shape-optimized isotropic case; a compliance of 1.377 and 1.209 and an energy concentration of 1.222 and 1.138. The shape itself has a sharper corner, with a volume (without the "arms") decrease to 62%.

Finally, the two bottom pictures in Fig. 13 are results for a material with extremely low stiffness in the vertical direction and in shear, being only 12.5% of the isotropic values. The results show the same tendencies as for the other examples, i.e. *by removing material in an optimal manner, we can diminish the energy concentration but at the expense of increasing the compliance.*

7 Conclusions

With models of a short cantilever, a biaxially loaded hole, a corner loaded square, and a cross connection problem, the paper shows computational results of optimal design; optimal in the sense that the stiffness of the continuum and/or the strength of the continuum is maximized. The study includes the material orientation for orthotropic materials, the thickness or density distribution for a given amount of material, and the shape of boundaries. Procedures based on optimality criteria are used, and only single

load cases are involved. The main goal of the study is to see the possibilities and limitations of the individual design variables and combinations of them.

For thickness (density) design we obtain continua of uniform energy density, at least within the limits set by the given minimum and maximum thicknesses. The optimal designs are obtained in 10–20 iterations with a well-known and simple recursive formula. With a uniform energy density we have both the stiffest and also the strongest continuum. It is a characteristic that these designs are tapered, and this might be a problem in some manufacturing cases.

In a specific example we therefore force the design to be non-tapered by a simple penalization approach (also well-known) and show the relations between the tapered and so-called "black and white" design, for which severe energy concentration may be the price that is paid for obtaining a design that is better suited to manufacturing.

For orientational design with orthotropic materials we obtain alignment of the numerically larger principal stress direction and the direction of the most stiff material direction. We use 10–20 iterations where the local (element) material is oriented with the current principal stress direction, and simultaneous thickness redesign also works without problems. The orientational optimization increases the stiffness (often significantly), but the diminishment of the energy concentration is not so large. Thus combined thickness and orientational optimal design is necessary for the strength optimization. Orthotropic materials are often more flexible in shear. We note that regions of pure shear stress tends to disappear as a result of the design for maximum stiffness.

Even without thickness and orientational design, by shape design of a hole boundary, we can obtain uniform energy density along the boundary, and in this way optimize the stiffness and the strength of the continuum. The shape design is strongly influenced by the level of orthotropy.

When the amount of material is not given, as in the example with shape design for a connection in a cross problem, then optimal design for stiffness and for strength have different solutions. Better stiffness is obtained with a more massive connection, while energy concentrations can be diminished by removing material, just like for fillet problems. In combination with orientational design for an orthotropic material, results of a parametric study are presented.

Acknowledgements For helpful suggestions on improving the manuscript, I wish to thank Martin P. Bendsøe of the Department of Mathematics, and Niels Olhoff and Niels L. Pedersen, both at the Institute of Mechanical Engineering, Aalborg University. I am also grateful for the comments of the unknown reviewer.

References

Bendsøe, M.P.; Sigmund, O. 2003: *Topology optimization – theory, methods and applications*. Springer

Cheng, G.; Pedersen, P. 1997: On sufficiency conditions for optimal design based on extremum principles of mechanics. *J. Mech. Phys. Solids* **45**(1), 135–150

Eschenauer, H.A.; Olhoff, N. 2001: Topology optimization of continuum structures – a review. *Appl. Mech. Rev.* **54**, 331–390

Gürdal, Z.; Haftka, R.T.; Hajela, P. 1999: *Design and optimization of laminated composite materials*. Wiley Chichester

Haftka, R.T.; Gurdal, Z.; Kamat, M.P. 1990: *Elements of structural optimization*. Kluwer

Pedersen, P.; Tobiesen, L.; Jensen, S.H. 1992: Shapes of orthotropic plates for minimum energy concentration. *Mech. Struct. Mach.* **20**(4), 499–514

Pedersen, P. 1989: On optimal orientation of orthotropic materials. *Struct. Optim.* **1**, 101–106

Pedersen, P. 1998: Some general optimal design results using anisotropic power law non-linear elasticity. *Struct. Optim.* **15**, 73–80

Pedersen, P. 2000: On optimal shapes in materials and structures. *Struct. Optim.* **19**, 169–182

Pedersen, P. 2001: On the influence of boundary conditions, Poisson's ratio and material non-linearity on the optimal shape. *Int. J. Solids Struct.* **38**(3), 465–477

Rozvany, G.I.N. 1989: *Structural design via optimality criteria*. Dordrecht: Kluwer